A finite volume-complete flux scheme for the singularly perturbed generalized Burgers-Huxley equation

EINDHOVEN UNIVERSITY OF TECHNOLOGY
Department of Mathematics and Computer Science

CASA-Report 16-15
June 2016

A Finite Volume-Complete Flux Scheme for the Singularly Perturbed Generalized Burgers-Huxley Equation

by

M.F.P. ten Eikelder, J.H.M. ten Thije Boonkkamp, B.V. Rathish Kumar

Centre for Analysis, Scientific computing and Applications
Department of Mathematics and Computer Science
Eindhoven University of Technology
P.O. Box 513
5600 MB Eindhoven, The Netherlands
ISSN: 0926-4507

A Finite Volume-Complete Flux Scheme for the Singularly Perturbed Generalized Burgers-Huxley Equation

M.F.P. ten Eikelder[a,b,*], J.H.M. ten Thije Boonkkamp[a], B.V. Rathish Kumar[b]

[a] *Eindhoven University of Technology, Department of Mathematics and Computer Science, P.O. Box 513, 5600 MB Eindhoven, The Netherlands*
[b] *Department of Mathematics and Statistics, Indian Institute of Technology Kanpur, Kanpur 208016, India*

Abstract

In this paper the finite volume-complete flux scheme is proposed to numerically solve the generalized Burgers-Huxley equation. The scheme is applied in an iterative manner. Numerical computations are performed for traveling wave-type problems as a validation of the method. Convection-dominated problems are used to assess the method on boundary layers. The results are in good agreement with reference results.

Keywords: Generalized Burgers-Huxley equation, Boundary layer, Singularly perturbed equation, Convection-dominated problem, Complete flux scheme, Finite volume method

1. Introduction

The generalized Burgers–Huxley (GBH) equation can be used to model the interaction between reaction mechanisms, convection and diffusion [1], and is widely used in modeling nonlinear wave phenomena [2]. J. Satsuma [1] was the first to study this equation in 1987. Exact solutions of

*Corresponding author.
Present address: Delft University of Technology, Department of Mechanical, Maritime and Materials Engineering, P.O. Box 5, 2600 AA Delft, The Netherlands
Email address: m.f.p.teneikelder@tudelft.nl (M.F.P. ten Eikelder)

the Burgers-Huxley equation can be obtained with a Cole-Hopf transformation [3]. Solitary wave solutions can be obtained by using special nonlinear transformations, as described in [4]. Similarity reductions (also known as similarity solutions) of the Burgers' and Burgers-Huxley equations are obtained by P.G. Estevez [5]. Exact solutions of some special cases are derived in [6, 7].

The approaches mentioned above consider special cases of the GBH equation. No general approach of finding analytical solutions of nonlinear advection-diffusion-reaction equations exists, therefore numerical methods are of great importance. Various numerical approaches have been proposed by researchers to solve the GBH equation. Without trying to be complete, we mention some. The first one is the spectral collocation method. This method casts the GBH equation into a set of ordinary differential equations, has been used by Darvishi et al. [8] and Javidi et al. [9]. The Adomian decomposition method (ADM), which yields an analytical solution in the form of a rapidly converging series, is a popular numerical technique for the GBH equation [10–13]. Another commonly used approach is the variational iteration method (VIM) [14–16]. This method yields rapidly convergent successive approximations of the exact solution without any restrictive approximations. The VIM is very effective and convenient in comparison with the ADM [15]. Another class of methods is the homotopy perturbation method, which shows rapid convergence towards the exact solution [17]. A B-spline second order scheme is used by R. Mohammadi [18]. Also approaches using the more classical technique of finite difference methods (FDMs) have been proposed to numerically solve the GBH equation: An exponential FDM [19], and higher order methods [20, 21]. Another popular class of methods to solve the GBH equation are the differential quadrature methods [22, 23]. Here a combination of a polynomial-based differential quadrature method in space and a third-order total variation diminishing Runge-Kutta scheme in time has been used. Lastly, we mention the Haar wavelet method [24] and the differential transform method [25] that can be used to solve the GBH equation.

In this paper not only the GBH equation, but also the singularly perturbed GBH equation is considered. The singularly perturbed GBH which exhibits boundary layers has been studied by B.V. Kumar et al. [26]. They have used a three-step Taylor-Galerkin method, which is third-order accurate in time. Also D. Kamboj et al. [27] have numerically solved this equation using a VIM.

In this study, we propose to use a finite volume method for solving the

GBH equation: the so-called finite volume-complete flux (FV-CF) scheme. The scheme, developed by Ten Thije Boonkkamp et al. [28], deals with linear advection-diffusion-reaction equations. It is based on an integral representation of the flux from the solution of a local boundary value problem of the entire equation. This means that the source term is included and, therefore, the flux consists of a homogeneous and an inhomogeneous part, corresponding to the homogeneous and particular solution of the boundary value problem, respectively. The latter part is of great importance when advection dominates diffusion. Due to the non-linearity of the GBH equation, the original scheme is applied in an iterative procedure. Traveling wave-problems are used to validate the method. The method is assessed for highly convection dominated problems with sharp boundary layer profiles. The proposed method is a simple and accurate approach to solve the GBH equation and can deal with boundary layers problems.

The outline of the paper is as follows. The nonlinear GBH equation is briefly presented in Section 2. In Section 3 the proposed FV-CF scheme is elaborated. Numerical results are presented in Section 4. Finally, the conclusions are drawn in Section 5.

2. The generalized Burgers-Huxley equation

The generalized Burgers-Huxley equation is a nonlinear partial differential equation (PDE) of second order. It differs from the well-known Burgers' equation by its highly nonlinear right-hand side. It describes the evolution of a wave profile $\varphi = \varphi(x,t)$ and reads

$$\begin{aligned} \partial_t \varphi + \alpha \varphi^\delta \partial_x \varphi - \varepsilon \partial_{xx} \varphi &= s(\varphi), \\ s(\varphi) &= \beta \varphi (1-\varphi^\delta)(\varphi^\delta - \gamma), \end{aligned} \tag{1}$$

where $t > 0$ denotes the time parameter and x the spatial coordinate. The second term on the left-hand side represents the nonlinear advection effect with advection speed α and the third term the diffusion with diffusion coefficient $\varepsilon > 0$. The source term s includes the strength β and the nonlinear perturbation parameter $0 < \gamma < 1$. The nonlinearity of the equation, caused by the parameter $\delta \geq 0$, vanishes for the choice $\delta = 0$ for which a homogeneous linear second order PDE is obtained. Note that for $\beta = 0, \delta = 1$, a zero right-hand side, the viscous Burgers' equation is retrieved. This equation has

an explicit family of traveling waves given by

$$\varphi = \tilde{\varphi}_{\kappa,c}(x,t) = \frac{c}{\alpha} - 2\kappa \tanh\left(\kappa\frac{\alpha}{\varepsilon}\big(x-\xi t\big)\right), \tag{2}$$

with $\kappa, \xi \in \mathbb{R}$. This is a stationary solution along the characteristic lines $x - \xi t =$ constant.

3. Numerical scheme

In this section we outline the finite volume-complete flux scheme for equations with a linear advection-diffusion operator; for more details see [28]. Next, we present the extension to a nonlinear advection term, as occurs in the (generalized) Burgers-Huxley equation.

First, we present the stationary flux approximation, thus we consider the model equation (conservation law)

$$\frac{\mathrm{d}f}{\mathrm{d}x} = s, \quad f = u\varphi - \varepsilon\frac{\mathrm{d}\varphi}{\mathrm{d}x}, \tag{3}$$

where f is the flux. Parameters in (3) are the advection velocity u and the diffusion coefficient $\varepsilon \geq \varepsilon_{\min} > 0$, both assumed to be sufficiently smooth functions of x, and $s = s(\varphi)$ is a (possibly nonlinear) source term. To discretize equation (3) we introduce an equidistant grid $x_j = (j-1)\Delta x\,(j = 1, 2, \ldots, N)$ with $\Delta x = L/(N-1)$ the grid size and N the number of grid points. Furthermore, we cover the domain with control volumes $\Omega_j = (x_{j-1/2}, x_{j+1/2})\,(j = 2, 3, \ldots, N-1)$ where $x_{j\pm1/2} = \frac{1}{2}(x_j + x_{j\pm1})$. Integrating the first equation in (3) over the control volume Ω_j and using the midpoint rule for the integral of the source term s, the discrete conservation law is obtained

$$F_{j+1/2} - F_{j-1/2} = s_j\,\Delta x, \tag{4}$$

where $F_{j+1/2}$ is the numerical flux at $x_{j+1/2}$ and $s_j = s(\varphi_j)$. The expression for the numerical flux $F_{j+1/2}$ is based on the following local boundary value problem

$$\frac{\mathrm{d}f}{\mathrm{d}x} = \frac{\mathrm{d}}{\mathrm{d}x}\left(u\varphi - \varepsilon\frac{\mathrm{d}\varphi}{\mathrm{d}x}\right) = s, \quad x_j < x < x_{j+1}, \tag{5a}$$

$$\varphi(x_j) = \varphi_j, \quad \varphi(x_{j+1}) = \varphi_{j+1}. \tag{5b}$$

Note that we consider the *entire* equation, including the source term, consequently, the numerical flux is the superposition of a homogeneous flux,

corresponding to the advection-diffusion operator, and an inhomogeneous flux, corresponding to the source term. Introducing the Péclet function P, defined as

$$P = \frac{u\Delta x}{\varepsilon}, \tag{6}$$

the expressions for the numerical flux read

$$F_{j+1/2} = F^{\mathrm{h}}_{j+1/2} + F^{\mathrm{i}}_{j+1/2}, \tag{7a}$$

$$F^{\mathrm{h}}_{j+1/2} = \frac{\bar{\varepsilon}_{j+1/2}}{\Delta x}\big(B(-\bar{P}_{j+1/2})\varphi_j - B(\bar{P}_{j+1/2}\varphi_{j+1}\big), \tag{7b}$$

$$F^{\mathrm{i}}_{j+1/2} = \big(\tfrac{1}{2} - W(\bar{P}_{j+1/2})\big)s_{\mathrm{u},j+1/2}\Delta x. \tag{7c}$$

In (7) the functions B and W are defined as

$$B(z) = \frac{z}{\mathrm{e}^z - 1}, \quad W(z) = \frac{\mathrm{e}^z - 1 - z}{z\big(\mathrm{e}^z - 1\big)}, \tag{8}$$

moreover, $\bar{P}_{j+1/2} = \frac{1}{2}\big(P_j + P_{j+1}\big)$ is the average Peclet number, and $s_{\mathrm{u},j+1/2}$ is the upwind value for s at the cell interface $x_{j+1/2}$. We refer to the flux approximation in (7) as the complete flux (CF) scheme.

Next, we consider the time-dependent version of equation (3), which reads

$$\frac{\partial\varphi}{\partial t} + \frac{\partial f}{\partial x} = s, \quad f = u\varphi - \varepsilon\frac{\partial\varphi}{\partial x}, \tag{9}$$

with corresponding semi-discrete conservation law

$$\dot{\varphi}_j\,\Delta x + F_{j+1/2} - F_{j-1/2} = s_j\,\Delta x, \tag{10}$$

where $\dot{\varphi}_j \approx \partial\varphi/\partial t(x_j, t)$. For the numerical flux we have two options. First, the flux approximation (7) can be taken, henceforth referred to as the stationary complete flux (SCF) scheme. The alternative is to include the time derivative in the source term, thus we introduce the modified source $\hat{s}$, defined as

$$\hat{s} = s - \frac{\partial\varphi}{\partial t}, \tag{11}$$

and replace $s_{\mathrm{u},j+1/2}$ in (7c) by $\hat{s}_{\mathrm{u},j+1/2}$. The inhomogeneous flux then changes to

$$F^{\mathrm{i}}_{j+1/2} = \big(\tfrac{1}{2} - W(\bar{P}_{j+1/2})\big)\big(s_{\mathrm{u},j+1/2} - \dot{\varphi}_{\mathrm{u},j+1/2}\big)\Delta x, \tag{12}$$

where $\dot{\varphi}_{\mathrm{u},j+1/2}$ denotes the upwind value of $\partial\varphi/\partial t$ at the interface $x_{j+1/2}$. Obviously, the homogeneous flux remains the same. We refer to this flux approximation as the transient complete flux (TCF) scheme.

Combining the semi-discrete conservation law (10) with the expressions for the numerical flux, we obtain the (implicit) ODE-system

$$\boldsymbol{M}\dot{\boldsymbol{\varphi}} + \boldsymbol{A}\boldsymbol{\varphi} = \boldsymbol{B}\boldsymbol{s} + \boldsymbol{b}, \tag{13}$$

where $\boldsymbol{A}$ and $\boldsymbol{B}$ represent the homogeneous and inhomogeneous flux differences, respectively. Furthermore, $\boldsymbol{M} = \Delta x\boldsymbol{I}$ for the SCF scheme and $\boldsymbol{M} = \boldsymbol{B}$ for the TCF scheme. Boundary conditions are incorporated in the right-hand side vector $\boldsymbol{b}$. For time integration of (13) the θ-method is used, which reads

$$\frac{1}{\Delta t}\boldsymbol{M}\big(\boldsymbol{\varphi}^{n+1}-\boldsymbol{\varphi}^{n}\big)+(1-\theta)\boldsymbol{A}\boldsymbol{\varphi}^{n}+\theta\boldsymbol{A}\boldsymbol{\varphi}^{n+1} = (1-\theta)\big(\boldsymbol{B}\boldsymbol{s}^{n}+\boldsymbol{b}^{n}\big)+\theta\big(\boldsymbol{B}\boldsymbol{s}^{n+1}+\boldsymbol{b}^{n+1}\big), \tag{14}$$

where $\boldsymbol{\varphi}^n \approx \boldsymbol{\varphi}(t_n)$, $t_n = n\Delta t\,(n = 0, 1, 2, \ldots)$ with $\Delta t > 0$ the time step and $\theta = 1/2$ for the second order accuracy [29].

The generalized Burgers-Huxley equation can be written as an nonlinear advection-diffusion-reaction equation:

$$\begin{aligned} \partial_t\varphi + v(\varphi)\partial_x\varphi - \varepsilon\partial_{xx}\varphi &= s(\varphi), \\ v = v(\varphi) &= \alpha\varphi^{\delta}, \end{aligned} \tag{15}$$

where v is the nonlinear advection term. In the same manner as in the linear case, we define now the nonlinear flux

$$\begin{aligned} f &= f(\varphi) = u\varphi - \varepsilon\frac{\partial\varphi}{\partial x}, \\ u &= u(\varphi) = \frac{v}{\delta+1}. \end{aligned} \tag{16}$$

Obviously, the previous derivation doesn't hold anymore. To remedy this problem we embed the scheme (14) in an iterative scheme as follows. Let $\psi_j^{(k)}$ be the kth iterative approximation for φ_j^{n+1}. The iterative procedure to compute from current time level n the solution at the next time level φ_j^{n+1} now reads:

1. Set $\psi_j^{(0)} = \varphi_j^n$;

2. Compute the Péclet numbers: $P_j^{(k)} = u(\psi_j^{(k)})\Delta x/\varepsilon$
3. Compute the matrices $\boldsymbol{M} = \boldsymbol{M}(\psi_j^{(k)}), \boldsymbol{A} = \boldsymbol{A}(\psi_j^{(k)}), \boldsymbol{B} = \boldsymbol{B}(\psi_j^{(k)}), \boldsymbol{b} = \boldsymbol{b}(\psi_j^{(k)})$;
4. Solve (14) with the TCF scheme (using a Newton-Rhapson iterative solver) to find $\psi_j^{(k)}$;
5. Repeat until convergence (and set $k = k + 1$);
6. Set $\varphi_j^{n+1} = \psi_j^{(k)}$;

4. Numerical results

The initial boundary value problem (IBVP) under consideration is composed of (1) with initial condition

$$\varphi(x, 0) = \varphi_0(x), \quad 0 \leq x \leq 1, \tag{17}$$

and Dirichlet boundary conditions

$$\varphi(0, t) = \varphi_L(t), \quad \varphi(1, t) = \varphi_R(t), \quad t \geq 0. \tag{18}$$

First, we validate the proposed method for a traveling wave solution. Next, the boundary layer profiles are assessed.

4.1. Validation of method: Traveling wave problem

This problem serves as a validation of the proposed method. In this boundary value problem the initial condition

$$\varphi(x, 0) = \left(\frac{\gamma}{2} + \frac{\gamma}{2}\tanh(kx)\right)^{1/\delta} \tag{19}$$

and the boundary conditions

$$\begin{aligned} \varphi_L(t) &= \left(\frac{\gamma}{2} + \frac{\gamma}{2}\tanh(-kct)\right)^{1/\delta}, t \geq 0, \\ \varphi_R(t) &= \left(\frac{\gamma}{2} + \frac{\gamma}{2}\tanh\left(k(1-ct)\right)\right)^{1/\delta}, t \geq 0, \end{aligned} \tag{20}$$

are chosen (with $\epsilon = 1$) such that an exact solitary wave solution exists. The constants k, c are defined as, see e.g. [22],

$$\begin{aligned} k &= \frac{-\alpha\delta + \delta\sqrt{(\alpha^2 + 4\beta(1+\delta))}}{4(1+\delta)}\gamma, \\ c &= \frac{\gamma\alpha}{1+\delta} - \frac{(1+\delta-\gamma)(-\alpha + \sqrt{(\alpha^2 + 4\beta(1+\delta))})}{2(1+\delta)}, \end{aligned} \tag{21}$$

and the corresponding exact solution is given by

$$\varphi(x,t) = \left(\frac{\gamma}{2} + \frac{\gamma}{2}\tanh\left(k\left(x - ct\right)\right)\right)^{1/\delta}, \quad t \geq 0. \tag{22}$$

To illustrate the behavior of the solution, we show some traveling wave profiles (with a strong source) in Figure 1. These profiles are obtained on a course mesh of $N = 15$ mesh points and a temporal step size of $\Delta t = 10^{-4}$.

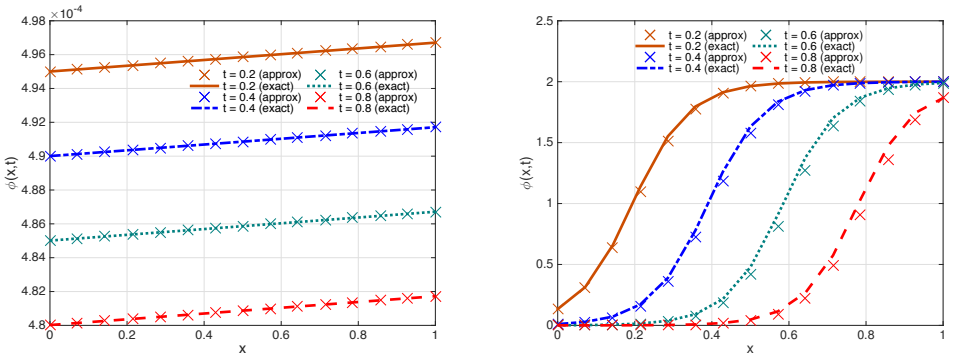

(a) (b)

Figure 1: Travelling wave - behavior of solution with strong source $\beta = 100$ and $\delta = \epsilon = 1$ with $N = 15$, $\Delta t = 10^{-4}$. Left panel: $\alpha = 1, \gamma = 10^{-3}$, right panel: $\alpha = 2, \gamma = 2$.

Evaluation at test bed

We evaluate the results of our scheme at the test bed of M. Sari et al. [22], which is, to the knowledge of the authors, the most complete testbed for the GBH equation in literature. We use *DQM-scheme* to refer to their method. The L_1-norm of the errors, referred to as *absolute errors*, at various grid points x_j and times t are computed. The results for various values of α, β, δ and γ are shown for four cases in Tables 1-5.

Case (i). We start off with a case with the parameters $\alpha = 1, \beta = 1$ and $\gamma = 10^{-3}$. In Table 1 we show the absolute errors of both schemes for various values of x, t and δ. A more nonlinear advection term, i.e. a higher δ, increases the complexity of the PDE. This is indicated by the results in the table: the errors declining increase for increasing δ. All errors of our scheme

are of the same magnitude as of the DQM scheme.

Case (ii). In this case we take a very weak source term, $\beta = 10^{-3}$, a small advection speed $\alpha = 10^{-1}$, and a small perturbation $\gamma = 10^{-4}$. This case can be considered as the simplest one of all considered test cases. We show the results for various values of x, t and δ in Table 2. Again, the errors declinningly increase for increasing δ. In all cases our scheme is about one order of magnitude more accurate than the DQM scheme.

Case (iii). Next, we take a negative advection speed, $\alpha = -10^{-1}$, a weak source term $\beta = 10^{-1}$, and a perturbation of $\gamma = 10^{-3}$. As in the previous two cases we vary δ and show the results for different values of x, t in Table 3. Again, the errors declinningly increase for increasing δ. Comparing with the results of the DQM scheme, the current errors are about a factor 2 smaller in middle of the grid and are of the same magnitude at the boundaries.

Case (iv). A strong source term of $\beta = 1, 10, 50, 100$ is taken in this case, which makes it a difficult one. The convection term is the same as for the Burgers' equation, $\delta = 1$, and the other parameter values are $\alpha = 1$ and $\gamma = 10^{-3}$. Table 4 shows the obtained results for various values of x, t and β. For both methods, the errors linearly increase for increasing β. Again, the comparison with the results of the DQM scheme shows that the current errors are about a factor 2 smaller in middle of the grid and are of the same magnitude at the boundaries.

Case (v). To check the influence of the perturbation parameter γ, we vary $\gamma = 10^{-2}, 10^{-3}, 10^{-4}, 10^{-5}$. A large perturbation γ is the most challenging case of this test bed. The other parameters are: a large advection speed of $\alpha = 5$, a strong source strength of $\beta = 10$ and a value of $\delta = 2$. Table 5 shows the absolute errors for various values of γ, x and t. For both methods, the errors increase for increasing γ. The comparison with the DQM scheme shows that the absolute errors of the current approach are of the same magnitude in the middle of the grid and are about a factor 2 larger at the boundaries.

x_i	t	$\delta=1$		$\delta=2$		$\delta=4$		$\delta=8$	
		FVCF	DQM	FVCF	DQM	FVCF	DQM	FVCF	DQM
	0.2	$1.982e-8$	$6.841e-9$	$8.106e-7$	$3.194e-7$	$5.091e-6$	$2.239e-6$	$1.248e-5$	$6.058e-6$
x_3	0.6	$1.483e-8$	$7.733e-9$	$6.586e-7$	$3.610e-7$	$4.381e-6$	$2.531e-6$	$1.128e-5$	$6.842e-6$
	0.8	$1.452e-8$	$7.748e-9$	$6.481e-7$	$3.617e-7$	$4.326e-6$	$2.535e-6$	$1.116e-5$	$6.852e-6$
	0.2	$4.258e-8$	$3.644e-8$	$1.727e-6$	$1.701e-6$	$1.078e-5$	$1.193e-5$	$2.627e-5$	$3.226e-5$
x_7	0.6	$3.091e-8$	$4.226e-8$	$1.371e-6$	$1.973e-6$	$9.117e-6$	$1.383e-5$	$2.346e-5$	$3.739e-5$
	0.8	$3.018e-8$	$4.236e-8$	$1.347e-6$	$1.977e-6$	$8.988e-6$	$1.386e-5$	$2.319e-5$	$3.746e-5$
	0.2	$2.778e-8$	$1.420e-8$	$1.132e-6$	$6.630e-7$	$7.096e-6$	$4.649e-6$	$1.736e-5$	$1.257e-5$
x_{13}	0.6	$2.057e-8$	$1.615e-8$	$9.127e-7$	$7.538e-7$	$6.070e-6$	$5.284e-6$	$1.562e-5$	$1.428e-5$
	0.8	$2.011e-8$	$1.618e-8$	$8.975e-7$	$7.553e-7$	$5.990e-6$	$5.294e-6$	$1.546e-5$	$1.431e-5$

Table 1: The absolute errors for various values of δ, x, and t with $\alpha=1, \beta=1$ and $\gamma=10^{-3}$.

x_i	t	$\delta=1$		$\delta=2$		$\delta=4$		$\delta=8$	
		FVCF	DQM	FVCF	DQM	FVCF	DQM	FVCF	DQM
	0.1	$9.549e{-}15$	$4.059e{-}14$	$1.350e{-}12$	$5.984e{-}12$	$1.606e{-}11$	$7.554e{-}11$	$5.538e{-}11$	$2.802e{-}10$
x_3	0.5	$1.435e{-}14$	$5.888e{-}14$	$2.029e{-}12$	$8.681e{-}12$	$2.413e{-}11$	$1.096e{-}10$	$8.323e{-}11$	$4.065e{-}10$
	1.0	$1.444e{-}14$	$5.924e{-}14$	$2.042e{-}12$	$8.733e{-}12$	$2.428e{-}11$	$1.102e{-}10$	$8.377e{-}11$	$4.090e{-}10$
	0.1	$1.855e{-}14$	$2.021e{-}13$	$2.624e{-}12$	$2.979e{-}11$	$3.120e{-}11$	$3.760e{-}10$	$1.076e{-}10$	$1.395e-9$
x_7	0.5	$2.977e{-}14$	$3.215e{-}13$	$4.211e{-}12$	$4.741e{-}11$	$5.008e{-}11$	$5.984e{-}10$	$1.727e{-}10$	$2.220e-9$
	1.0	$2.998e{-}14$	$3.239e{-}13$	$4.241e{-}12$	$4.775e{-}11$	$5.043e{-}11$	$6.027e{-}10$	$1.740e{-}10$	$2.236e-9$
	0.1	$1.293e{-}14$	$8.301e{-}14$	$1.828e{-}12$	$1.224e{-}11$	$2.173e{-}11$	$1.545e{-}10$	$7.496e{-}11$	$5.731e{-}10$
x_{13}	0.5	$1.986e{-}14$	$1.229e{-}13$	$2.809e{-}12$	$1.812e{-}11$	$3.340e{-}11$	$2.288e{-}10$	$1.152e{-}10$	$8.487e{-}10$
	1.0	$1.999e{-}14$	$1.237e{-}13$	$2.827e{-}12$	$1.824e{-}11$	$3.362e{-}11$	$2.302e{-}10$	$1.160e{-}10$	$8.541e{-}10$

Table 2: The absolute errors for various values of δ, x, and t with $\alpha=10^{-1}, \beta=10^{-3}$ and $\gamma=10^{-4}$.

x_i	t	$\delta = 1$		$\delta = 2$		$\delta = 4$		$\delta = 8$	
		FVCF	DQM	FVCF	DQM	FVCF	DQM	FVCF	DQM
	0.3	$2.338e-9$	$2.317e-9$	$9.792e-8$	$1.013e-7$	$6.277e-7$	$6.628e-7$	$1.577e-6$	$1.682e-6$
x_4	0.5	$2.087e-9$	$2.413e-9$	$9.180e-8$	$1.055e-7$	$6.075e-7$	$6.902e-7$	$1.560e-6$	$1.751e-6$
	0.9	$2.002e-9$	$2.428e-9$	$8.949e-8$	$1.062e-7$	$5.982e-7$	$6.944e-7$	$1.546e-6$	$1.762e-6$
	0.3	$3.684e-9$	$6.580e-9$	$1.535e-7$	$2.878e-7$	$9.805e-7$	$1.882e-6$	$2.457e-6$	$4.776e-6$
x_8	0.5	$3.259e-9$	$6.899e-9$	$1.431e-7$	$3.017e-7$	$9.464e-7$	$1.974e-6$	$2.429e-6$	$5.007e-6$
	0.9	$3.115e-9$	$6.950e-9$	$1.392e-7$	$3.039e-7$	$9.306e-7$	$1.988e-6$	$2.406e-6$	$5.043e-6$
	0.3	$2.872e-9$	$3.695e-9$	$1.200e-7$	$1.616e-7$	$7.684e-7$	$1.057e-6$	$1.928e-6$	$2.681e-6$
x_12	0.5	$2.555e-9$	$3.855e-9$	$1.123e-7$	$1.686e-7$	$7.430e-7$	$1.103e-6$	$1.908e-6$	$2.798e-6$
	0.9	$2.447e-9$	$3.881e-9$	$1.094e-7$	$1.697e-7$	$7.311e-7$	$1.110e-6$	$1.890e-6$	$2.816e-6$

Table 3: The absolute errors for various values of δ, x, and t with $\alpha = -10^{-1}, \beta = 10^{-1}$ and $\gamma = 10^{-3}$.

x_i	t	$\beta = 1$		$\beta = 10$		$\beta = 50$		$\beta = 100$	
		FVCF	DQM	FVCF	DQM	FVCF	DQM	FVCF	DQM
	0.3	$1.608e-8$	$1.545e-8$	$1.607e-7$	$1.854e-7$	$8.036e-7$	$9.807e-7$	$1.607e-6$	$1.989e-6$
x_4	0.5	$1.917e-8$	$1.608e-8$	$1.917e-7$	$1.930e-8$	$9.583e-7$	$1.021e-8$	$1.915e-6$	$2.071e-8$
	0.9	$1.997e-8$	$1.618e-8$	$1.607e-7$	$1.942e-7$	$8.036e-7$	$1.027e-6$	$1.607e-6$	$2.082e-6$
	0.3	$2.447e-8$	$4.387e-8$	$2.447e-7$	$5.264e-7$	$1.223e-6$	$2.785e-6$	$2.446e-6$	$5.649e-6$
x_8	0.5	$2.971e-8$	$4.387e-8$	$2.971e-7$	$5.520e-7$	$1.485e-6$	$2.920e-6$	$2.968e-6$	$5.922e-6$
	0.9	$3.106e-8$	$4.633e-8$	$3.105e-7$	$5.560e-7$	$1.552e-6$	$2.941e-6$	$3.098e-6$	$5.960e-6$
	0.3	$1.949e-8$	$2.463e-8$	$1.948e-7$	$2.956e-7$	$9.740e-7$	$1.564e-6$	$1.948e-6$	$3.172e-6$
x_12	0.5	$2.340e-8$	$2.570e-8$	$2.340e-7$	$3.084e-7$	$1.170e-6$	$1.632e-6$	$2.338e-6$	$3.309e-6$
	0.9	$2.441e-8$	$2.587e-8$	$2.440e-7$	$3.105e-7$	$1.219e-6$	$1.642e-7$	$2.434e-6$	$3.328e-6$

Table 4: The absolute errors for various values of β, x, and t with $\alpha = 1$ and $\gamma = 10^{-3}$.

x_i	t	$\gamma = 10^{-2}$		$\gamma = 10^{-3}$		$\gamma = 10^{-4}$		$\gamma = 10^{-5}$	
		FVCF	DQM	FVCF	DQM	FVCF	DQM	FVCF	DQM
	0.3	$4.081e-4$	$2.039e-4$	$1.334e-5$	$6.505e-6$	$4.231e-7$	$2.059e-7$	$1.338e-8$	$6.512e-9$
x_4	0.5	$2.931e-4$	$2.116e-4$	$9.955e-6$	$6.771e-6$	$3.167e-7$	$2.144e-7$	$1.002e-8$	$6.780e-9$
	0.9	$2.316e-4$	$2.111e-4$	$8.851e-6$	$6.808e-6$	$2.837e-7$	$2.157e-7$	$8.982e-9$	$6.823e-9$
	0.3	$6.536e-4$	$5.809e-4$	$2.135e-5$	$1.848e-5$	$6.774e-7$	$5.848e-7$	$2.143e-8$	$1.849e-8$
x_8	0.5	$4.600e-4$	$6.071e-4$	$1.563e-5$	$1.937e-5$	$4.973e-7$	$6.131e-7$	$1.573e-8$	$1.939e-8$
	0.9	$3.596e-4$	$6.064e-4$	$1.377e-5$	$1.950e-5$	$4.414e-7$	$6.175e-7$	$1.398e-8$	$1.953e-8$
	0.3	$5.049e-4$	$3.268e-4$	$1.649e-5$	$1.083e-5$	$5.231e-7$	$3.283e-7$	$1.655e-8$	$1.083e-8$
x_12	0.5	$3.588e-4$	$3.399e-4$	$1.221e-5$	$1.083e-5$	$3.885e-7$	$3.426e-7$	$1.229e-8$	$1.083e-8$
	0.9	$2.816e-4$	$3.392e-4$	$1.082e-5$	$1.089e-5$	$3.468e-7$	$3.426e-7$	$1.098e-8$	$1.091e-8$

Table 5: The absolute errors for various values of β, x, and t with $\alpha = 5$ and $\beta = 10, \delta = 2$.

4.2. Boundary layer problem

In this case we asses the scheme on problems with sharp boundary layers. The initial boundary value problem consists of Eq. (1) with initial and boundary conditions

$$\begin{aligned} \varphi_0(x) &= \sin(\pi x), \\ \varphi_L(t) &= 0, \qquad 0 \le t \le 1, \\ \varphi_R(t) &= 0, \qquad 0 \le t \le 1. \end{aligned} \tag{23}$$

We start off by presenting a grid validation of the method. The two different sets of parameters which are used for this propose are given in Table 6.

Table 6: Boundary layer problem - Parameters for the grid validation.

	α	β	γ	δ	ϵ
Set 1	1	1	10^{-3}	2	2^{-7}
Set 2	10	100	10^{-3}	1	2^{-3}

The numerical simulations are performed using the double mesh principle with grid sizes $\Delta x = 2^{-6}, 2^{-7}, 2^{-8}, 2^{-9}$. The solutions are evaluated using a temporal step size of $\Delta t = 10^{-3}$. We show the obtained solution profiles in Figure 2.

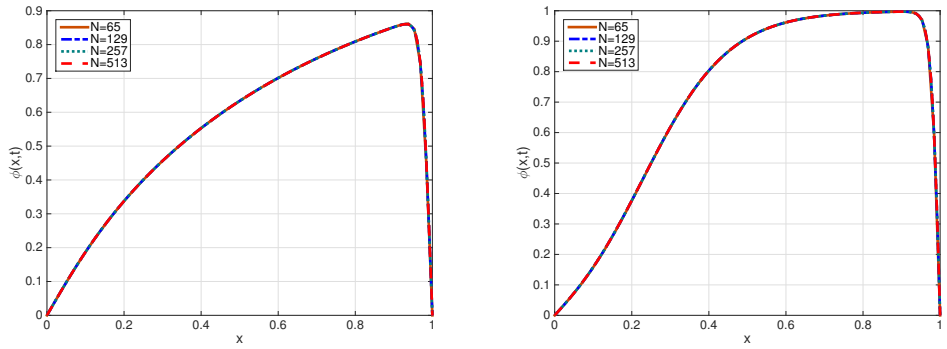

(a) (b)

Figure 2: Boundary layer problem - A grid validation. The left (right) panel shows the numerical results for parameter set 1 (2).

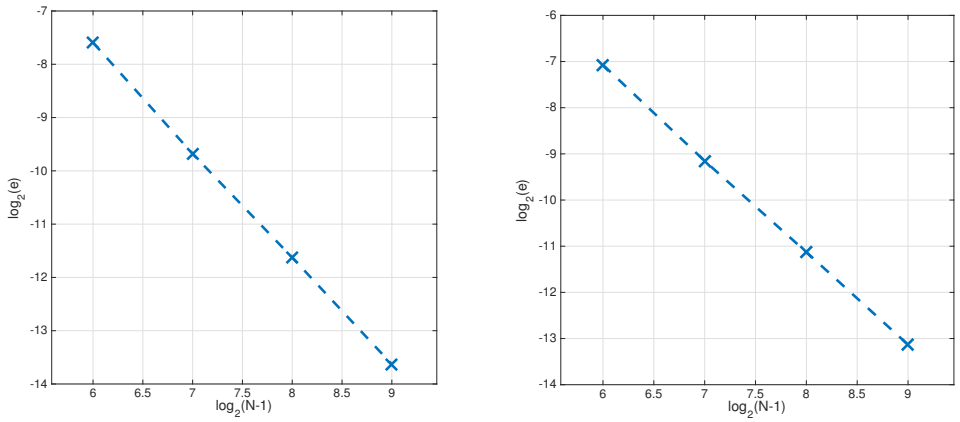

(a) (b)

Figure 3: Boundary layer problem - The maximum absolute errors for various meshes.

In Figure 2 no difference between the profiles is visible, which indicates the same behavior of the solutions for $N > 65$. We performing all remaining computations with $N = 129$.

Since the exact solution for this IBVP is unknown, we use the solution at a very fine mesh ($\Delta x = 2^{-15}$) as a reference solution. The maximum absolute error, denoted e, is computed for the various meshes and is visualized in Figure 3. To find the spatial accuracy, we compute $\varphi(x_M, \frac{1}{2})$ for decreasing grid sizes and apply Richardson extrapolation [30] to the results, where x_M is the middle gridpoint. For the size of the time steps we take $\Delta t = 10^{-4}$. Let $\varphi_{\Delta x}$ be the numerical solution at $x = x_M$ and $t = 1.0$ respectively, computed with grid size Δx. Furthermore, let $e_{\Delta x}$ be the error corresponding to the $\varphi_{\Delta x}$, i.e.

$$\varphi_{\Delta x} + e_{\Delta x} = \varphi_{\Delta x/2} + e_{\Delta x/2} = \varphi_{\Delta x/4} + e_{\Delta x/4}, \tag{24}$$

We now assume

$$e_h = Ch^p + \mathcal{O}\left(h^q\right), \tag{25}$$

where $q \in \mathbb{N}, q > p$ and the order of convergence can be estimated:

$$2^p \doteq \frac{\varphi_{\Delta x/2} - \varphi_{\Delta x}}{\varphi_{\Delta x/4} - \varphi_{\Delta x/2}} =: r_{\Delta x}, \tag{26}$$

We show the $r_{\Delta x}$-values in Table 7.

Table 7: Boundary layer problem - Parameters for the grid validation.

Δx	2^{-6}	2^{-7}	2^{-8}	2^{-9}
Set 1	4.030	4.013	4.006	4.003
Set 2	3.746	3.862	3.928	3.963

Figure 3 and Table 7 indicate, for both parameter sets, quadratic convergence for decreasing mesh size of the solution to the reference solution.

We assess the method for the boundary layer development ($\epsilon \to 0$) using the same parameters as in [26]: $\alpha = 1, \beta = 1, \gamma = 0.001, \delta = 1, 2, 3$. The solutions are evaluated at the time levels $t = 0.4$ and $t = 0.8$. The positive advection speed α and the small diffusion coefficient ϵ (formally a large Péclet number) in combination with the boundary condtions enforce the formation of the boundary layer, as depicted in Figure 4.

The plots in Figure 4 indicate that the method can deal with (very) sharp boundary layers. A comparison with the results in [26] shows no visible difference between the both methods.

We close this section by showing the boundary layer formation for increasing t in Figure 5. Again, there is no visible difference between our method and the one in [26].

5. Summary and Conclusions

In this paper we have applied the finite volume-complete flux scheme to the singularly perturbed generalized Burgers-Huxley equation. The equation is approached in an advection-diffusion-reaction fashion with nonlinear advection. The integral representation of a linear advection-diffusion-reaction equation, including source term, is used. As a result, the numerical flux consists of a homogeneous and an inhomogeneous part, of which the latter has proven to be very important for highly convection dominated problems. The transient complete flux scheme is used, which is very suitable for these problems. Furthermore, the scheme shows quadratic convergence for finer meshes and has only a three-point spatial coupling.

The method is successfully validated on a large test bed of parameter values. To assess the ability of the current method on boundary layer containing profiles, highly advection dominated problems have been accurately solved. The boundary layers have been captured very accurately and are

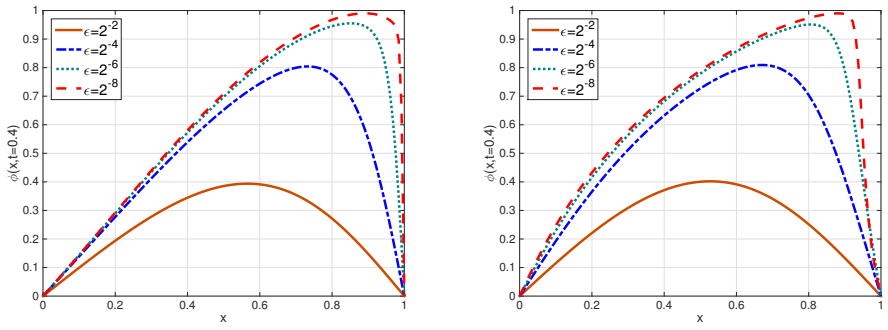

(a) $\delta = 1, t = 0.4$ (b) $\delta = 2, t = 0.4$

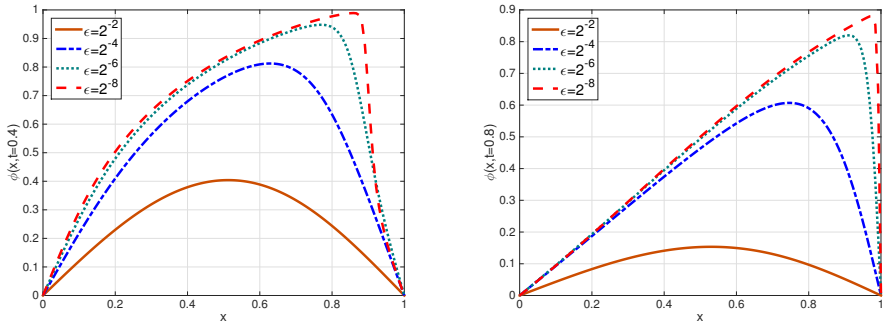

(c) $\delta = 3, t = 0.4$ (d) $\delta = 1, t = 0.8$

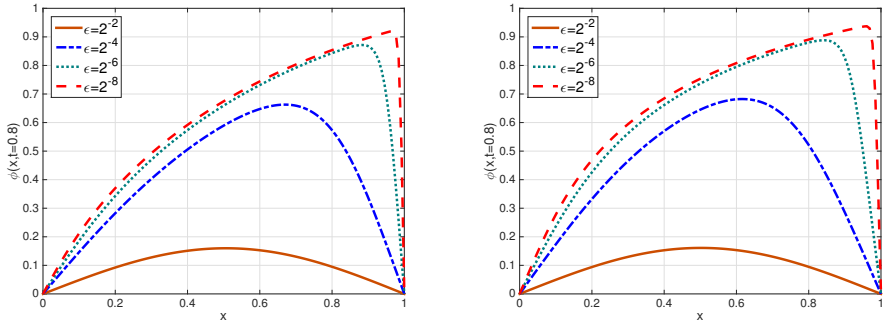

(e) $\delta = 2, t = 0.8$ (f) $\delta = 3, t = 0.8$

Figure 4: Boundary layer problem - The evolution of a boundary layer as $\epsilon \to 0$. In each one of these simulations we take $\alpha = 1, \beta = 1, \gamma = 0.001$ and vary δ and t.

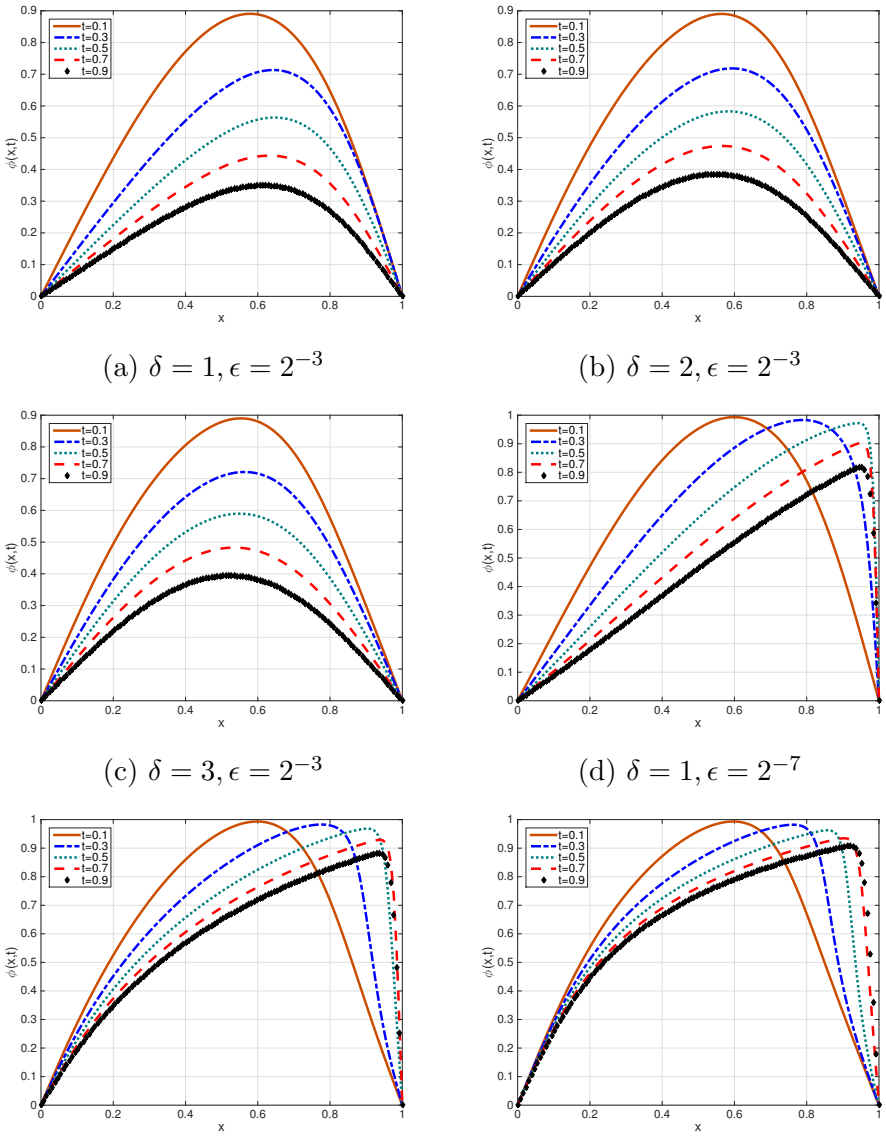

(a) $\delta = 1, \epsilon = 2^{-3}$ (b) $\delta = 2, \epsilon = 2^{-3}$

(c) $\delta = 3, \epsilon = 2^{-3}$ (d) $\delta = 1, \epsilon = 2^{-7}$

(e) $\delta = 2, \epsilon = 2^{-7}$ (f) $\delta = 3, \epsilon = 2^{-7}$

Figure 5: Boundary layer problem - Formation of a boundary layer. In each one of these simulations we take $\alpha = 1, \beta = 1, \gamma = 0.001$ and vary δ and ϵ.

in perfect agreement with reference results. Furthermore, the results never show spurious oscillations or under or overshooting.

References

[1] J. Satsuma, M. Ablowitz, B. Fuchssteiner, M. Kruskal, Topics in soliton theory and exactly solvable nonlinear equations, World Scientific, Singapore, 1987.

[2] A.-M. Wazwaz, Travelling wave solutions of generalized forms of Burgers, Burgers–KdV and Burgers–Huxley equations, Applied Mathematics and Computation 169 (2005) 639–656.

[3] O. Y. Yefimova, N. Kudryashov, Exact solutions of the Burgers–Huxley equation, Journal of Applied Mathematics and Mechanics 68 (2004) 413–420.

[4] X. Y. Wang, Z. S. Zhu, Y. K. Lu, Solitary wave solutions of the generalised Burgers-Huxley equation, Journal of Physics A: Mathematical and General 23 (1990) 271–274.

[5] P. G. Estevez, Non-classical symmetries and the singular manifold method: the Burgers and the Burgers–Huxley equations, Journal of Physics A: Mathematical and General 27 (1994) 2113–2127.

[6] H. Gao, R. X. Zhao, New exact solutions to the generalized Burgers–Huxley equation, Applied Mathematics and Computation 217 (2010) 1598–1603.

[7] G. W. Wang, X. Q. Liu, Y. Y. Zhang, New xxplicit solutions of the generalized Burgers–Huxley equation, Vietnam Journal of Mathematics 41 (2013) 161–166.

[8] M. T. Darvishi, S. Kheybari, F. Khani, Spectral collocation method and Darvishi's preconditionings to solve the generalized Burgers–Huxley equation, Communications in Nonlinear Science and Numerical Simulation 13 (2008) 2091–2103.

[9] M. Javidi, A numerical solution of the generalized Burgers–Huxley equation by spectral collocation method, Applied Mathematics and Computation 178 (2006) 338–344.

[10] I. Hashim, M. S. M. Noorani, M. R. S. Al-Hadidi, Solving the generalized Burgers–Huxley equation using the Adomian decomposition method, Mathematical and Computer Modelling 43 (2006) 1404–1411.

[11] I. Hashim, M. S. M. Noorani, B. Batiha, A note on the Adomian decomposition method for the generalized Huxley equation, Applied Mathematics and Computation 181 (2006) 1439–1445.

[12] A. M. Al-Rozbayani, M. Al-Amr, Discrete Adomian decomposition method for solving Burgers-Huxley Equation, Int. J. Contemp. Math. Sciences 813 (2013) 623–631.

[13] M. Javidi, A. Golbabai, A new domain decomposition algorithm for generalized Burgers–Huxley equation based on Chebyshev polynomials and preconditioning, Chaos, Solitons & Fractals 39 (2009) 849–857.

[14] B. Batiha, M. S. M. Noorani, I. Hashim, Numerical simulation of the generalized Huxley equation by He's variational iteration method, Applied Mathematics and Computation 186 (2007) 1322–1325.

[15] B. Batiha, M. S. M. Noorani, I. Hashim, Application of variational iteration method to the generalized Burgers–Huxley equation, Chaos, Solitons & Fractals 36 (2008) 660–663.

[16] A. J. Khattak, A computational meshless method for the generalized Burgers–Huxley equation, Applied Mathematical Modelling 33 (2009) 3718–3729.

[17] S. S. Nourazar, M. Soori, A. Nazari-Golshan, On the exact solution of Burgers–Huxley equation using the homotopy perturbation method, Journal of Applied Mathematical Physics 3 (2015) 285–294.

[18] R. Mohammadi, B-spline collocation algorithm for numerical solution of the generalized Burgers–Huxley equation, Numerical Methods for Partial Differential Equations 29 (2013) 1173–1191.

[19] B. İnan, A. Bahadir, Numerical solutions of the generalized Burgers-Huxley equation by implicit exponential finite difference method, Journal of Applied Mathematics, Statistics and Informatics 11 (2015) 57–67.

[20] M. Sari, G. Gürarslan, A. Zeytinoğlu, High-order finite difference schemes for numerical solutions of the generalized Burgers–Huxley equation, Numerical Methods for Partial Differential Equations 27 (2011) 1313–1326.

[21] A. G. Bratsos, et al., A fourth order improved numerical scheme for the generalized Burgers–Huxley equation, American Journal of Computational Mathematics 1 (2011) 152–158.

[22] M. Sari, G. Gürarslan, Numerical solutions of the generalized Burgers–Huxley equation by a differential quadrature method, Mathematical Problems in Engineering 2009.

[23] M. Sari, Differential quadrature solutions of the generalized Burgers-Fisher equation with a strong stability preserving high-order time integration, Mathematical and Computational Applications 16 (2011) 477–486.

[24] İ. Çelik, Haar wavelet method for solving generalized Burgers–Huxley equation, Arab Journal of Mathematical Sciences 18 (2012) 25–37.

[25] J. Biazar, F. Mohammadi, Application of differential transform method to the generalized Burgers–Huxley equation, Applications and Applied Mathematics: An International Journal 5 (2010) 1726–1740.

[26] B. V. Rathish Kumar, V. Sangwan, S. V. S. S. N. V. G. K. Murthy, M. Nigam, A numerical study of singularly perturbed generalized Burgers–Huxley equation using three-step Taylor–Galerkin method, Computers & Mathematics with Applications 62 (2011) 776–786.

[27] D. Kamboj, M. D. Sharma, Singularly perturbed Burgers-Huxley equation: Analytical solution through iteration, International Journal of Engineering, Science and Technology 5 (2013) 45–57.

[28] J. H. M. ten Thije Boonkkamp, M. J. H. Anthonissen, The finite volume-complete flux scheme for advection-diffusion-reaction equations, Journal of Scientific Computing 46 (2011) 47–70.

[29] M. F. P. ten Eikelder, J. H. M. ten Thije Boonkkamp, M. P. T. Moonen, B. V. Rathish Kumar, A finite volume-complete flux scheme for a polluted groundwater site, CASA-Report 15-11, 2015.

[30] A. Quarteroni, R. Sacco, F. Saleri, Numerical Mathematics, Vol. 37, Springer Science & Business Media, 2010.

PREVIOUS PUBLICATIONS IN THIS SERIES:

Number	Author(s)	Title	Month
16-11	B. Plestenjak M.E. Hochstenbach	Roots of bivariate polynomial systems via determinantal representations	May ‘16
16-12	P.G.Th. van der Varst A.A.F. van de Ven G. de With	Load-depth sensing of isotropic, linear viscoelastic materials using rigid axisymmetric indenters	May ‘16
16-13	S.W. Rienstra	Sound Propagation in Slowly Varying 2D Duct with Shear Flow	May ‘16
16-14	A.S. Tijsseling Q. Hou Z. Bozkuş	Analytical and numerical solution for a rigid liquid-column moving in a pipe with fluctuating reservoir-head and venting entrapped-gas	May ‘16
16-15	M.F.P. ten Eikelder, J.H.M. ten Thije Boonkkamp, B.V. Rathish Kumar	A Finite Volume-Complete Flux Scheme for the Singularly Perturbed Generalized Burgers-Huxley Equation	June ‘16

Ontwerp: de Tantes,
Tobias Baanders, CWI